CCSN and AGB Star Yields of Nitrogen

Core-Collapse Supernova Yields

Empirically, nitrogen-to-oxygen ratios exhibit a plateau at log(N/O) ≈ -1.5 for log(O/H) $\lesssim$ 8 (see Fig. 1 of Vincenzo et al., 2016 comparing Berg et al., 2012, Izotov, Thuan & Guseva, 2012, and James et al., 2015 measurements).

What is the implied relation between the IMF integrated CCSN yields of nitrogen and oxygen?

The ratio of their yields can be related to the number densities of the two nuclei in the supernova ejecta via:

$$\frac{y_{\rm N}^{\rm CC}}{y_{\rm O}^{\rm CC}} = \frac{\mu_{\rm N} n_{\rm N}}{\mu_{\rm O} n_{\rm O}} \tag{1}$$

where μ_x is the mean molecular weight of a species x and n_x is the number of nuclei. Taking the ratio $n_{\rm N}/n_{\rm O}$ from these observed results yields:

$$\frac{y_{\rm N}^{\rm CC}}{y_{\rm O}^{\rm CC}} = \frac{\mu_{\rm N}}{\mu_{\rm O}} 10^{\log({\rm N/O})} \tag{2}$$

Though supernova ejecta may produce different isotopic ratios of N than AGB stars, potentially altering the ratio $\mu_{\rm N}/\mu_{\rm O}$, taking $\mu_{\rm N} = 14.007$ and $\mu_{\rm O} = 15.999$ from a periodic table suggests that, with the previously adopted $y_{\rm O}^{\rm CC} = 0.015$ (e.g. Weinberg, Andrews & Freudenburg, 2017; Johnson & Weinberg, 2020; Johnson et al., 2021), this suggests

$$y_{\rm N}^{\rm CC} = \frac{\mu_{\rm N}}{\mu_{\rm O}} 10^{\log({\rm N/O})} y_{\rm O}^{\rm CC} = \frac{14.007}{15.999} 10^{-1.5} (0.015) \approx 4.15 \times 10^{-4} \tag{3}$$

Can this be understood from theoretically predicted yields?

The left panel of Figure 1 presents the IMF-integrated yields $y_{\rm N}^{\rm CC}$ computing with VICE using the Limongi & Chieffi (2018), Sukhbold et al. (2016), Nomoto et al. (2013), and Woosley & Weaver (1995) CCSN yield tables, with Limongi & Chieffi (2018) being the only study which reports yields for rotating progenitors. Broadly, the non-rotating predictions are consistent with one another, and predict a significant metallicity dependence; the lowest metallicity progenitor from Woosley & Weaver (1995) predict somewhat higher yields overall, but this could have to do with this being the only yield set for which we can calculate only *gross* yields rather than *net* yields. The rotating progenitors from Limongi & Chieffi (2018), however, predict that the yield should be considerably enhanced by rotation. They interpret this as being due to the interplay between the core helium and hydrogen burning shells triggered by rotation-induced instabilities, which drives the synthesis of all products of CNO, not just ^{14}N (see their abstract). These yields predict a relatively metallicity-independent $y_{\rm N}^{\rm CC}$ of $\sim 5\times10^{-4}$, in surprisingly good agreement with the empirically derived value of 4.15×10^{-4}.

The right panel of Figure 1 presents the IMF-integrated nitrogen-to-oxygen ratios predicted by the same studies for the same combinations of metallicity and rotational velocity. The flat, dotted black line denotes $\log_{10}({\rm N/O})_{\rm CC}$ = -1.5, the value empirically derived from observations (Vincenzo et al., 2016; Berg et al., 2012; Izotov et al., 2012; James et al., 2015).

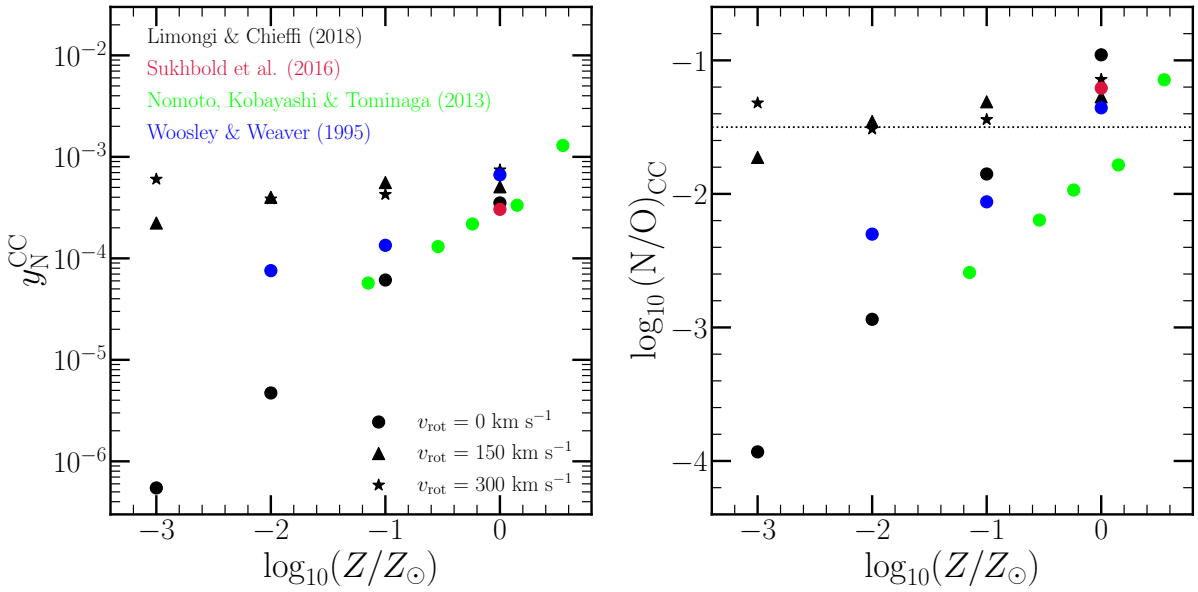

Figure 1: **Right**: IMF-integrated CCSN yields of N computed with VICE using the Limongi & Chieffi (2018) (black), Sukhbold et al. (2016) (crimson), Nomoto et al. (2013) (lime), and Woosley & Weaver (1995) (blue) yield sets. **Left**: IMF-integrated nitrogen-to-oxygen yield ratios computed with VICE for the same studies. The Limongi & Chieffi (2018) yields are calculated with progenitor rotational velocities of $v_{\rm rot} = 0$ (circles), 150 (triangles), and 300 km/s (stars). All other studies only report yields for non-rotating progenitors.

The rotating progenitor models from Limongi & Chieffi (2018) do the best job of reproducing this ratio in theoretical models of core collapse supernova ejecta; the other models do not include rotation, which appears to play a key role in establishing this empirical result.

What is the implied plateau in [N/O]?
[N/O] and log(N/O) are directly related, but one is relative to the sun while the other is just a ratio of number densities. Expanding [N/O]:

$$[\rm N/O] = [\rm N/H] - [\rm O/H] \tag{4a}$$
$$= \log_{10}\left(\frac{Z_{\rm N}}{Z_{\rm N,\odot}}\right) - \log_{10}\left(\frac{Z_{\rm O}}{Z_{\rm O,\odot}}\right) \tag{4b}$$
$$= \log_{10}\left(\frac{Z_{\rm N}}{Z_{\rm O}}\right) - \log_{10}\left(\frac{Z_{\rm N,\odot}}{Z_{\rm O,\odot}}\right) \tag{4c}$$

Zooming in on the $Z_{\rm N}/Z_{\rm O}$ term:

$$\log_{10}\left(\frac{Z_{\rm N}}{Z_{\rm O}}\right) = \log_{10}\left(\frac{\mu_{\rm N} n_{\rm N}}{\mu_{\rm O} n_{\rm O}}\right) \tag{5a}$$
$$= \log_{10}\left(\frac{\mu_{\rm N}}{\mu_{\rm O}}\right) + \log_{10}\left(\frac{n_{\rm N}}{n_{\rm O}}\right) \tag{5b}$$

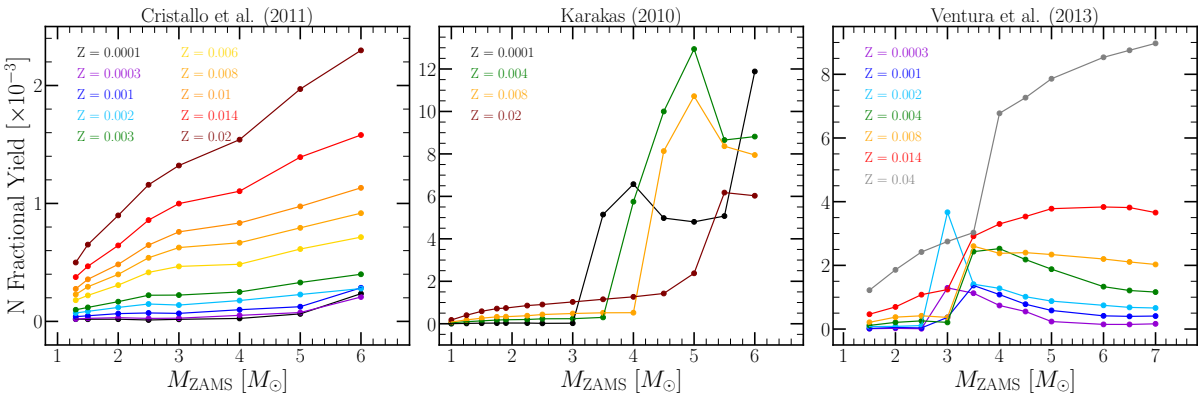

Figure 2: Fractional yields of N as a function of progenitor zero age main sequence mass at the metallicities at which Cristallo et al. (2011) (left), Karakas (2010) (middle), and Ventura et al. (2013) (right) report yields.

where μ and n are again the mean molecular weight and number of some species x. The term $\log_{10}(n_{\rm N}/n_{\rm O})$ is exactly the log(N/O) value which Berg et al. (2012), Izotov, Thuan & Guseva (2012), and James et al. (2015) measured to be ∼-1.5. Plugging this in:

$$[{\rm N/O}] = \log_{10}\left(\frac{\mu_{\rm N}}{\mu_{\rm O}}\right) + \log_{10}\left(\frac{n_{\rm N}}{n_{\rm O}}\right) - \log_{10}\left(\frac{Z_{\rm N,\odot}}{Z_{\rm O,\odot}}\right) \tag{6a}$$

Taking $\mu_{\rm N} = 14.007$ and $\mu_{\rm O} = 15.999$ again, with the empirical result of $\log_{10}(n_{\rm N}/n_{\rm O}) = $ -1.5 and the Asplund et al. (2009) solar photospheric composition of $Z_{\rm N,\odot} = 6.91\times10^{-4}$ and $Z_{\rm O,\odot} = 0.00572$, yields the following:

$$[{\rm N/O}]_{\rm plateau} = -0.64 \tag{7}$$

Asymptotic Giant Branch Star Yields

Figure 2 presents the fractional yields of N as a function of progenitor zero age main sequence (ZAMS) mass and metallicity as reported in the FRUITY database (Cristallo et al., 2011, 2015, left), by Karakas (2010) (middle), and by Ventura et al. (2013) (right). All models predict a metallicity dependence to the nitrogen yields, though with noticeably different dependencies; both Cristallo et al. (2011, 2015) and Ventura et al. (2013) predict the yields to increase more or less linearly with progenitor metallicity, whereas the Karakas (2010) yields predict higher N yields at lower metallicities for higher mass AGB stars. This is a consequence of the interplay between third dredge up (TDU) and hot bottom burning (HBB) in these models.

TDU refers to the repeated penetrations of the convective envelope into the hydrogen depleted core during the thermal pulses associated with AGB star evolution. This process is particularly important in low mass AGB stars whose main source of neutrons is the ^{13}C(α, n)^{16}O reaction, which can occur at substantial rates when C is mixed with material from the He-rich shell during each TDU episode. At solar metallicity, Karakas (2010) suggests that only stars with $M_{\rm ZAMS} \gtrsim 2.5\ M_\odot$ are massive enough to experience TDU, though the threshold is as low as $\sim 1\ M_\odot$ at $Z \approx 10^{-4} Z_\odot$; lower mass stars instead experience only a core

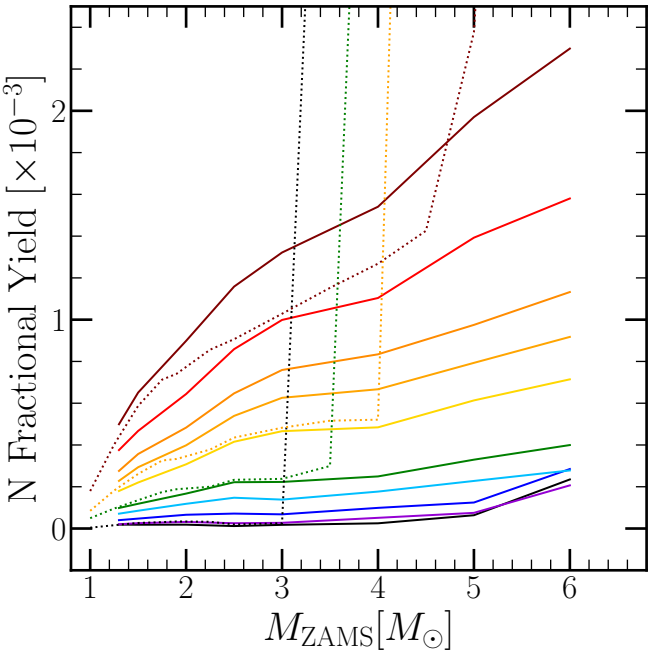

Figure 3: The same as figure 2, but with the Cristallo et al. (2011) (solid) and Karakas (2010) (dotted) yields plotted on the same set of axes for comparison.

helium flash. HBB refers to proton captures at the base of the convective envelope, which activates the CNO cycle, producing large amounts of ^{13}C and ^{14}N. It requires temperatures of at least 30-40 MK according to Ventura et al. (2013), but 80 MK according to Cristallo et al. (2015). HBB requires a higher mass AGB progenitor (∼4 - 5 $M_{\odot}$), but like TDU, the minimum mass also decreases at lower progenitor metallicity. The CNO cycle:

^{12}C(p,γ)^{13}N(β^{+}, ν_e)^{13}C(p,γ)^{14}N(p,γ)^{15}O(β^{+}, ν_e)^{15}N(p,α)^{12}C

The most efficient N production thus occurs when an AGB star experiences *both* TDU and HBB, because each TDU episode adds more C and N seed nuclei with which to conduct p-capture nucleosynthesis. This is the reason the Karakas (2010) N yields are so high at high masses: every massive star in their model experiences both TDU and HBB, whereas the Ventura et al. (2013) models have both only in the ∼3 - 4 $M_{\odot}$ range (hence the enhanced N yields there). The Cristallo et al. (2011) paper makes no mention of HBB, but my impression from Cristallo et al. (2015) is that their $M > 4$ $M_{\odot}$ models all have both TDU and HBB implemented, though in most cases one is much more efficient than the other. The metallicity dependence of the N yields reported by Karakas (2010) therefore reflect the fact that low-Z models experience deeper TDU and stronger HBB (see discussion in § 4.1 of Ventura et al., 2013). Beyond this, a direct comparison of the models is significantly challenging (and even avoided by mose of the papers which publish them) owing to the laundry list of assumptions that go into the stellar models: the treatment of convection and convective boundaries, the mass-loss rate, opacities, the equation of state, the nuclear reaction network, etc.

How consistent are Cristallo et al. (2011, 2015) and Karakas (2010) up to ∼3 - 4 $M_\odot$? Figure 3 compares the two sets of yields on the same plot, with the Cristallo et al. (2011, 2015) set shown in solid lines and the Karakas (2010) set in dotted lines. The two are broadly consistent with one another up to this threshold mass, at which point HBB takes hold in the Karakas (2010) model, significantly enhancing the N yields for higher mass progenitors.

Analytic Motivation of Nitrogen Yields

Can we come up with a mathematical framework with which to relate a late-time [N/O]-[O/H] relation and nitrogen yields using equilibrium arguments in simple one-zone models?

The time-derivative of the main sequence mass fraction

The main sequence mass fraction is the fraction of a stellar population's mass still on the main sequence. If the post-main sequence lifetime is approximated to be zero, this is also the star cluster mass fraction. It is given by:

$$h = \frac{\int_l^{m_{\rm to}} m \frac{dN}{dm} dm}{\int_l^u m \frac{dN}{dm} dm}, \tag{8}$$

where l and u are the lower and upper mass limits on star formation, respectively, dN/dm is the adopted stellar IMF, and $m_{\rm to}$ is the turnoff mass in solar masses. Allowing the constant ξ to represent the normalization of the IMF, zooming in on the denominator:

$$\int_l^u = \xi m^{1-\alpha} dm \tag{9a}$$

$$= \frac{\xi}{2-\alpha} m^{2-\alpha}\Big|_l^u \tag{9b}$$

$$= \frac{\xi}{0.7} m^{0.7}\Big|_{0.08}^{0.5} - \frac{\xi}{0.6} m^{-0.3}\Big|_{0.5}^{100} \tag{9c}$$

$$= 2.239\xi \tag{9d}$$

where the power-law indeces and constants are appropriate for a Kroupa (2001) IMF (with 0.6 in the second denominator rather than 0.3 to account for piece-wise continuity) assuming l = 0.08 and u = 100. In the numerator of h, only the quantity $m_{\rm to}$ varies with time. The time-derivative then follows trivially from the stellar IMF.

$$\dot{h} = \frac{1}{2.239\xi} \frac{d}{dt} \int_l^{m_{\rm to}} m \frac{dN}{dm} dm \tag{10a}$$

$$= \frac{1}{2.239\xi} \frac{d}{dm_{\rm to}} \int_l^{m_{\rm to}} m \frac{dN}{dm} dm \frac{dm_{\rm to}}{dt} \tag{10b}$$

$$= \frac{m_{\rm to}}{2.239\xi} \frac{dN}{dm}\Big|_{m_{\rm to}} \frac{dm_{\rm to}}{dt} \tag{10c}$$

$$= \frac{m_{\rm to}}{2.239\xi} A\xi m_{\rm to}^{-\alpha} \frac{dm_{\rm to}}{dt} \tag{10d}$$

where $\alpha = 1.3$ (2.3) for $0.08 \leq m \leq 0.5$ ($m \geq 0.5$) according to the Kroupa (2001) IMF and $A = 1$ (0.5) for the same mass ranges ensures piece-wise continuity of the IMF. However, since the lifetime of an $m = 0.5$ star is very long (∼113 Gyr for `VICE`'s approximation), $A = 0.5$ and $\alpha = 2.3$ always for the sake of this calculation.

$$= \frac{0.5 m_{\rm to}}{2.239\xi} \xi m_{\rm to}^{-2.3} \frac{dm_{\rm to}}{dt} \tag{11a}$$

$$= 0.223 m_{\rm to}^{-1.3} \frac{dm_{\rm to}}{dt} \tag{11b}$$

The turnoff mass at a given time, as approximated in `VICE`, is given by

$$m_{\rm to} = \left(\frac{t}{\tau_\odot}\right)^{-1/3.5} = \left(\frac{t}{\tau_\odot}\right)^{-2/7}, \tag{12}$$

where $\tau_\odot$ is the main sequence lifetime of the sun. Differentiating with time:

$$\frac{dm_{\rm to}}{dt} = \frac{-2}{7\tau_\odot}\left(\frac{t}{\tau_\odot}\right)^{-9/7} \tag{13}$$

Plugging equations 12 and 13 into equation 11b:

$$\dot{h} = 0.223 \left(\frac{t}{\tau_\odot}\right)^{2.6/7} \left(\frac{-2}{7\tau_\odot}\right) \left(\frac{t}{\tau_\odot}\right)^{-9/7} \tag{14a}$$

$$= \frac{-0.0637}{\tau_\odot}\left(\frac{t}{\tau_\odot}\right)^{-6.4/7} \tag{14b}$$

$$= \frac{-0.0637}{\tau_\odot}\left(\frac{t}{\tau_\odot}\right)^{-32/35} \tag{14c}$$

This form for $\dot{h}$ is appropriate for the Kroupa (2001) IMF with a mass range of star formation defined by $l = 0.08$ and $u = 100$ assuming a mass-lifetime relationship given by 12. However, the time-dependence is set not by the IMF but by the mass-lifetime relationship; the IMF affects only the normalization of $\dot{h}$.

The Enrichment Rate from AGB Stars

Next, equation 14c must be plugged into the equation describing the enrichment rate from AGB stars:

$$\dot{M}_{\rm N}^{\rm AGB} = -\int_0^T y_{\rm N}^{\rm AGB}(m_{\rm to}(T-t), Z_{\rm ISM}(t))\dot{M}_\star(t)\dot{h}(T-t)dt \tag{15}$$

In general, the SFR $\dot{M}_\star$ can have any time-dependence, and the gas-phase abundance of the star forming reservoir $Z_{\rm ISM}$ as a function of time has some complicated form which depends on the SFH. As a first guess though, we can assume a constant SFR, and since nitrogen production is dominated by young stellar populations, most of the enrichment should be coming from stars near the equilibrium abundance. Furthermore, the AGB star yields of N appear to depend more or less linearly on initial stellar mass. As a first guess then, assume

that $y_{\rm N}^{\rm AGB} = \xi m_{\rm to} Z$ where ξ is simply a normalizing constant. Under these assumptions this integral can be re-expressed as:

$$\dot{M}_{\rm N}^{\rm AGB} = -\int_0^T \xi m_{\rm to}(T-t) Z_{\rm eq} \dot{M}_\star \dot{h}(T-t) dt \tag{16a}$$

$$= \xi Z_{\rm eq} \dot{M}_\star \int_0^T \left(\frac{T-t}{\tau_\odot}\right)^{-2/7} \frac{0.0637}{\tau_\odot} \left(\frac{T-t}{\tau_\odot}\right)^{-6.4/7} dt \tag{16b}$$

$$= \frac{0.0637 \xi Z_{\rm eq} \dot{M}_\star}{\tau_\odot} \int_0^T \left(\frac{T-t}{\tau_\odot}\right)^{-8.4/7} dt \tag{16c}$$

$$= \frac{0.0637 \xi Z_{\rm eq} \dot{M}_\star}{\tau_\odot} \left[\left(\frac{-7}{1.4}\right)\left(\frac{T-t}{\tau_\odot}\right)^{-1.4/7} (-\tau_\odot)\right]_0^T \tag{16d}$$

$$= 0.3185 \xi Z_{\rm eq} \dot{M}_\star \left[\left(\frac{\tau_8}{\tau_\odot}\right)^{-1.4/7} - \left(\frac{T}{\tau_\odot}\right)^{-1.4/7}\right] \tag{16e}$$

$$= 0.3185 \xi Z_{\rm eq} \dot{M}_\star \left[\left(\frac{\tau_8}{\tau_\odot}\right)^{-1.4/7} - \left(\frac{T}{\tau_\odot}\right)^{-1.4/7}\right] \tag{16f}$$

$$= 1.064 \xi Z_{\rm eq} \dot{M}_\star \tag{16g}$$

In the second to last equality, the upper bound of the integral is evaluated at $T - \tau_8$ rather than inserting an infinity; mathematically, the infinite value reflects the divergence of $\dot{h}$ for zero-age stellar populations. However, the integral really should only be evaluated up to the simulation time minus the lifetime of an 8 $M_\odot$ star (τ_8), since these are the most massive AGB stars in these models. The final equality assumes a lifetime of $\tau_\odot 8^{-3.5}$ Gyr as the lifetime of an 8 $M_\odot$ star, $T = 13.2$ Gyr as the simulation time, and $\tau_\odot = 10$ Gyr as the lifetime of the sun.

The rate of CCSN enrichment reflects the yield at the equilibrium metallicity:

$$\dot{M}_{\rm N}^{\rm CC} = y_{\rm N}^{\rm CC}(Z_{\rm eq}) \dot{M}_\star \tag{17}$$

The Equilibrium Abundance of Nitrogen

The equilibrium metallicity for a constant SFH then corresponds to solving for $\dot{Z}_{\rm N} = 0$ from the following, derived from the enrichment equation and the equilibrium arguments from Weinberg, Andrews & Freudenburg (2017):

$$\dot{Z}_{\rm N} = \frac{1}{\dot{M}_\star \tau_\star}\left[\dot{M}_{\rm N}^{\rm CC} + \dot{M}_{\rm N}^{\rm AGB} - Z_{\rm N}\dot{M}_\star(1+\eta-r)\right] \tag{18}$$

When $\dot{Z}_{\rm N} = 0$, $Z_{\rm N} = Z_{\rm N,eq}$, the equilibrium abundance of nitrogen. It then follows:

$$Z_{\rm N,eq}\dot{M}_\star(1+\eta-r) = \dot{M}_{\rm N}^{\rm CC} + \dot{M}_{\rm N}^{\rm AGB} \tag{19a}$$

$$= y_{\rm N}^{\rm CC}(Z_{\rm eq})\dot{M}_\star + 1.064\xi Z_{\rm eq}\dot{M}_\star \tag{19b}$$

$$Z_{\rm N,eq} = \frac{y_{\rm N}^{\rm CC}(Z_{\rm eq}) + 1.064\xi Z_{\rm eq}}{1+\eta-r} \tag{19c}$$

Since nitrogen has metallicity dependent yields, $Z_{\rm eq}$ is the *total* abundance. The constant ξ specifies the normalization of the nitrogen AGB star yield assuming a linear dependence on both turnoff mass and metallicity given by $y_{\rm N}^{\rm AGB} = \xi m_{\rm to} Z$. This form does make the assumption that all AGB star production is coming from younger stellar populations near the equilibrium abundance. Since N production timescales are quite short ($\sim$100 Myr), this assumption is likely accurate enough. The constant ξ could be determined by a fit to the Cristallo et al. (2011) or the Ventura et al. (2013) models, also absorbing whatever prefactor is built in; the Karakas (2010) yields likely couldn't be used for this since they do not show a linear dependence of $y_{\rm N}^{\rm AGB}$ on progenitor mass.

The basic motivation of this is that at a given radius $R_{\rm gal}$, the equilibrium abundance of oxygen is known by the scaling of η to set the metallicity gradient. By assuming that the equilibrium abundance of nitrogen reflects the observed [N/O]-[O/H] relation, the only remaining unknowns in this formalism are the yields. This procedure can then be tested with `VICE`'s numerical simulations allowing migration, time-dependent SFHs, etc. to test how robust the predictions are to the assumptions built into this analytic argument.

Bibliography

Asplund M., Grevesse N., Sauval A. J., Scott P., 2009, ARA&A, 47, 481

Berg D. A., et al., 2012, ApJ, 754, 98

Cristallo S., et al., 2011, ApJS, 197, 17

Cristallo S., Straniero O., Piersanti L., Gobrecht D., 2015, ApJS, 219, 40

Izotov Y. I., Thuan T. X., Guseva N. G., 2012, A&A, 546, A122

James B. L., Koposov S., Stark D. P., Belokurov V., Pettini M., Olszewski E. W., 2015, MNRAS, 448, 2687

Johnson J. W., Weinberg D. H., 2020, MNRAS, 498, 1364

Johnson J. W., et al., 2021, arXiv e-prints, p. arXiv:2103.09838

Karakas A. I., 2010, MNRAS, 403, 1413

Kroupa P., 2001, MNRAS, 322, 231

Limongi M., Chieffi A., 2018, ApJS, 237, 13

Nomoto K., Kobayashi C., Tominaga N., 2013, ARA&A, 51, 457

Sukhbold T., Ertl T., Woosley S. E., Brown J. M., Janka H. T., 2016, ApJ, 821, 38

Ventura P., Di Criscienzo M., Carini R., D'Antona F., 2013, MNRAS, 431, 3642

Vincenzo F., Belfiore F., Maiolino R., Matteucci F., Ventura P., 2016, MNRAS, 458, 3466

Weinberg D. H., Andrews B. H., Freudenburg J., 2017, ApJ, 837, 183

Woosley S. E., Weaver T. A., 1995, ApJS, 101, 181